Journal of Nanobiotechnology

RESEARCH

Open Access

Probiotic-derived extracellular vesicles alleviate AFB1-induced intestinal injury by modulating the gut microbiota and AHR activation

Jinyan Li[1,2,3], Mengdie Shi[1,2,3], Yubo Wang[1,2,3], Jinyan Liu[1,2,3], Shuiping Liu[1,2,3], Weili Kang[1,2,3], Xianjiao Liu[1,2,3], Xingxiang Chen[1,2,3], Kehe Huang[1,2,3] and Yunhuan Liu[1,2,3*]

Abstract

Background Aflatoxin B1 (AFB1) is a mycotoxin that widely found in the environment and mouldy foods. AFB1 initially targets the intestine, and AFB1-induced intestinal injury cannot be ignored. *Lactobacillus amylovorus* (LA), a predominant species of *Lactobacillus*, plays a role in carbohydrate metabolism. Extracellular vesicles (EVs), small lipid membrane vesicles, are widely involved in diverse cellular processes. However, the mechanism by which *Lactobacillus amylovorus*-QC1H-derived EVs (LA.EVs) protect against AFB1-induced intestinal injury remains unclear.

Results In our study, a new strain named *Lactobacillus amylovorus*-QC1H (LA-QC1H) was isolated from pig faeces. Then, EVs derived from LA-QC1H were extracted via ultracentrifugation. Our results showed that LA.EVs significantly alleviated AFB1-induced intestinal injury by inhibiting the production of proinflammatory cytokines, decreasing intestinal permeability and increasing the expression of tight junction proteins. Moreover, 16 S rRNA analysis revealed that LA.EVs modulated AFB1-induced gut dysbiosis in mice. However, LA.EVs did not exert beneficial effects in antibiotic-treated mice. LA.EVs treatment increased intestinal levels of indole-3-acetic acid (IAA) and activated intestinal aryl hydrocarbon receptor (AHR)/interleukin-22 (IL-22) signalling in AFB1-exposed mice. Inhibition of intestinal AHR signalling markedly weakened the protective effect of LA.EVs in AFB1-exposed mice.

Conclusions LA.EVs alleviated AFB1-induced intestinal injury by modulating the gut microbiota, activating the intestinal AHR/IL-22 signalling, reducing the inflammatory response and promoting intestinal barrier repair in mice.

Keywords Aflatoxin B1, *Lactobacillus amylovorus*, Extracellular vesicles, Gut microbiota, Aryl hydrocarbon receptor

*Correspondence:
Yunhuan Liu
liuyunhuan@njau.edu.cn
[1]College of Veterinary Medicine, Nanjing Agricultural University, Nanjing, Jiangsu Province 210095, China
[2]Institute of Animal Nutritional Health, Nanjing Agricultural University, Nanjing, Jiangsu, China
[3]MOE Joint International Research Laboratory of Animal Health and Food Safety, College of Veterinary Medicine, Nanjing Agricultural University, Nanjing, Jiangsu, China

Background

Aflatoxin is a mycotoxin produced by *Aspergillus flavus*, *Aspergillus parasiticus*, and *Aspergillus nominus*. The most prevalent and toxic aflatoxin is aflatoxin B1(AFB1) [1]. AFB1 is listed as a class I carcinogen by the International Agency for Research on Cancer (IARC) in humans [2, 3]. AFB1 exposure can lead to many health issues through the food chain, including growth, gastrointestinal and reproductive system diseases [4, 5]. The target organ for AFB1 is the liver. However, orally ingested food first reaches the gastrointestinal tract [6]. Previous research has shown that AFB1 exposure can destroy the intestine by impairing the structure of the intestinal epithelium, suppressing tight junction protein expression, and increasing bacterial displacement [7, 8].

Lactobacillus amylovorus (LA), a lactic acid bacterium, can hydrolyse lake powder [9]. LA is often used as a silage fermentation additive in animal husbandry [10]. In the field of medicine, LA has been used to treat intestinal diseases in humans [11]. LA offers potential therapeutic strategy to prevent intestinal disorders in piglets and humans [12]. However, with the widespread use of antibiotics, the activity of probiotics has weakened. Recent research has shown that in both prokaryotes and higher eukaryotes, the exchange of cell biological signals is mainly mediated by the secretion of extracellular vesicles (EVs) [13]. EVs are nanosized vesicles that are released by all life domains [14]. Bacteria-derived EVs facilitate communication with host cells via pattern recognition receptors to activate signalling pathway [15]. It has been reported that *C. butyricum*-derived EVs upregulates gut barrier-related proteins to protect against dextran sodium sulfate (DSS)-induced colitis [16]. Increasing evidence has demonstrated the importance of bacterial EVs in intestinal homeostasis [17, 18]. However, whether LA.EVs can alleviate AFB1-induced intestinal injury is unknown.

The gut microbiota (GM) is composed of bacteria, protozoa, archaea, fungi and viruses and plays crucial roles in host health. Microbial disturbance leads to the occurrence of many intestinal disorders [19]. Previous research reports that the reversal of GM dysbiosis is essential for the effects of *C. butyricum*-derived EVs on ulcerative colitis (UC) [16]. Not only does the gut microbiota play the protective effect in host health, but also the gut microbial metabolites [20]. Gut microbial metabolites that are produced near the gut epithelium play important roles in gut barrier function. Aryl hydrocarbon receptor (AHR) has attracted increasing attention due to its role in the regulation of inflammation, immunity, intestinal barrier function, and intestinal microecology [21, 22]. Several studies have confirmed that inflammatory bowel disease (IBD) and colitis can be alleviated by AHR ligands through the activation of AHR [23, 24]. Notably, most microbial metabolites, including tryptophan metabolites, short-chain fatty acids and phenolic metabolites, are endogenous ligands of AHR present in the gastrointestinal tract [21, 25]. In particular, the tryptophan metabolite indole and its derivatives can regulate intestinal barrier function through AHR [26]. Indole-3-acetic acid (IAA), a tryptophan metabolite, can activate AHR to enhance the gut barrier function [27].

AHR, a ligand-activated multifunctional transcription factor [28], is expressed in various tissues and cells. Furthermore, there is evidence that AHR plays a key role in driving the production of interleukin-22 (IL-22) and regulating the development of Group 3 innate lymphoid cells (ILC3s) to control intestinal inflammation [29, 30]. And IL-22 can repair the intestinal barrier by increasing the expression of intestinal tight junction proteins and antimicrobial peptides [27]. Therefore, the activation of this pathway may be a novel alternative treatment for AFB1-induced intestinal injury.

In this study, we found that LA.EVs alleviated AFB1-induced intestinal injury by modulating the gut microbiota, increasing intestinal IAA levels and subsequently activating intestinal AHR/IL-22 signalling. This study provides new directions and targets for the treatment of AFB1-induced intestinal injury.

Materials and methods

Enrichment and isolation of *Lactobacillus amylovorus-QC1H* (LA-QC1H)

Several faeces samples (pigs) were collected from a local city (Nanjing, Jiangsu Province, China). Samples (0.3 g) were mixed with 3 mL of sterilized saline water. Then, 100 µL of the above suspensions was mixed with 900 µL of sterilized saline water to form gradient dilutions. Mixtures of 10^5, 10^6 and 10^7 were coated on DeMan, Rogosa and Sharpe (MRS) agar media and incubated at 37 °C for 48 h. Colonies of different shapes and sizes were chosen for streaking and purification. Milky white, prominent, and gram-positive strains were selected for identification and stored at -80 °C.

16 S rDNA sequencing

Genomic DNA was extracted using a bacterial genomic DNA extraction kit. The amplified products were subsequently sequenced by Sangon Biotech (Shanghai, China). Sequences showing more than 97% similarity to the 16 S rDNA gene of the isolated strains were identified, and phylogenetic trees were constructed.

LA culture and LA.EVs isolation

The strain was cultured in MRS broth at 37 °C for 48 h. Then, the bacterial solution was centrifuged at 10,000×g for 20 min after the bacterial cultures were pelleted. The obtained supernatants were filtered (0.22 µm) to remove

parental bacterial debris and other impurities. To generate crude EVs, the supernatant was further concentrated to 1/8, ultracentrifuged at 4 °C (5000×g, 25 min), and washed with PBS twice. The purified EVs were obtained by filtering (0.22 μm) again after ultracentrifugation at 160,000×g at 4 °C for 2 h.

Transmission electron microscopy (TEM)

Fifteen microlitres of EVs solution was dripped on a copper grid for 1 min, and then 2% uranyl acetate (15 μL) was applied to the grid for 1 min to conduct negative staining. Imaging was performed under a HITACHI HT7800 transmission electron microscope when the grids were completely dry.

Nanoparticle tracking analysis (NTA)

The sample was diluted in 1x PBS. When the number of exosome particles displayed in the instrument detection interface was between 50 and 400, the instrument started working automatically. The collected data for each sample were analysed with ZetaView.

Animals and experimental design

The study was approved by Nanjing Agricultural University under the Laboratory Animal Care Ethics Committee for Animal Experiments (NJAU. No 20210624093) before the study was initiated. Six to seven weeks old C57BL/6J male mice from GemPharmatech Co., Ltd. (Jiangsu, China) were randomly divided into different groups. All mice were fed a standard pellet diet and deionized water freely at a suitable temperature, humidity, and a 12 h light-dark cycle. AFB1 (Sigma) was dissolved in DMSO to prepare a stock solution of AFB1. Then, the AFB1 standard stock solution was diluted with olive oil as the working solution. The experimental design was as follows.

Experiment I

After acclimatization for one week, fifteen mice were randomly divided into the following groups (n=5): the control group (CON), AFB1 group (AFB1), and AFB1+LA.EVs group (AFB1+LA.EVs). AFB1 was orally administered to mice at 0.75 mg/kg BW once daily for 4 weeks. LA.EVs were administered to mice daily by gavage of 200 μL (25 μg protein content) for 4 weeks.

Experiment II

To explore the effect of gut microbes in the process of LA.EVs treatment, twenty mice were randomly assigned to the following groups (n=5): CON, AFB1, AFB1+LA.EVs and AFB1+LA.EVs+antibiotics (ABX) (AFB1+LA.EVs+ABX). AFB1 was orally administered to the mice at 0.75 mg/kg body weight (BW) once daily for 4 weeks. LA.EVs were administered to mice daily by gavage of 200 μL (25 μg protein content) for 4 weeks. Mice in AFB1+LA.EVs+ABX group were treated a cocktail of 10 mg of antibiotics (ampicillin, vancomycin, metronidazole, and neomycin) by oral gavage daily for seven days. Then fecal samples from mice were collected, homogenized, plated on Luria-Bertani agar and cultured at 37 °C for 2 d to confirm efficient depletions. On the eighth day, antibiotics (1 g/L for ampicillin, metronidazole, and neomycin and 500 mg/L for vancomycin) were added to the drinking water. And the antibiotics were maintained in the drinking water until the end of the entire experiment [31].

Experiment III

To explore the protective mechanism of LA.EVs on AFB1-induced intestinal inflammatory injury, twenty mice were randomly assigned to the following groups (n=5): CON, AFB1, AFB1+LA.EVs and AFB1+LA.EVs+CH223191 (AHR antagonist, Med Chem Express, NJ, USA) groups. AFB1 was orally administered to mice at 0.75 mg/kg BW once daily for 4 weeks. LA.EVs were administered to mice daily by gavage of 200 μL (25 μg protein content) for 4 weeks. CH223191 was administered to mice by intraperitoneal injection of 10 mg/kg BW once daily for 4 weeks.

On the 29th day, all mice were euthanized by CO_2 inhalation after weighing and then obtained the blood [32], and the supernatant was collected after centrifugation at 3000 rpm for 20 min. A portion of the ileum was harvested for haematoxylin-eosin (H&E) staining, and the remaining portion was placed at - 80 °C.

H&E staining

Ileum tissue samples were placed in 4% paraformaldehyde, fully fixed for 24 h, and then dehydrated with 70%, 80%, 90%, 95%, and 100% alcohol. Subsequently, the samples were soaked in xylene until they were cleared, and embedded in paraffin. The ileum tissues were then cut into 5 μm sections using a rotary microtome (Leica, Germany). After the sections were dried, they were stained with haematoxylin and eosin to assess tissue structure. The sections were observed using an optical microscope and photographed. The villus length was measured using ImageJ software.

Intestinal permeability assay

Mice were fasted for 4 h after FITC-dextran 4 kDa (FD-4) (Sigma–Aldrich, MO, USA) was administered orally (400 mg/kg). Then, the blood samples were harvested for isolation of serum. 10 μL of serum was used for FD-4 concentration measurement using a HITACHI F-7000 fluorimeter.

Immunofluorescence analysis

Zonula occludens-1 (ZO-1) and AHR protein expression in the ileum was analysed by immunofluorescence colocalization. Mouse ileum sections were incubated with anti-ZO-1 and anti-AHR antibodies at 4 °C overnight, followed by incubation with secondary antibodies. 4′,6-Diamidin-2-phenylindol (DAPI) was used to counterstain the nuclei for 10 min. Fluorescence images were obtained by an LSM710 immunofluorescence microscope (Carl Zeiss, Jena, Germany).

Real-time PCR

Total RNA from ileum tissues (0.02 g) was isolated using TRIzol Reagent (Accurate Biotechnology Co., Ltd., Hunan, China) following the manufacturer's instructions. An A260/A280 ratio of RNA between 1.8 and 2.0 indicated acceptable quality and integrity. The relative expression of target genes was calculated through the $2^{-\Delta\Delta Ct}$ approach and compared with that of GAPDH. All primers were synthesized by Sangon Biotech (Shanghai, China) and are listed in Table S1.

Western blotting

The ileum was dissolved in radioimmunoprecipitation assay (RIPA) lysis buffer supplemented with phenyl methyl sulphonyl fluoride (PMSF) to extract protein, and the protein concentration was quantified with a bicinchoninic acid (BCA) assay kit. Protein extracts were mixed with loading buffer (1: 4) and fully denatured in a metallic bath (95℃, 10 min). Total protein (30-50 μg) was added to the gels, and the separated protein was transferred to 0.45 μm polyvinylidene difluoride membranes (Millipore, MA, USA). The membranes were immersed in 5% bovine serum albumin (BSA) for 1.5 h at room temperature, wished with 1x TBST three times for six minutes each time on the shaking table, and then incubated with the primary antibody overnight at 4 °C. Finally, the membranes were incubated with the secondary antibody for 1 h at room temperature and washed with 1x TBST for three times on the shaking table. A Bio-Rad chemical imaging system was used to observe the protein bands. The expression levels of the indicated proteins were quantified digitally and normalized to the relative expression of GAPDH.

16 S rRNA gene sequencing

Approximately 0.5 g of faecal sample was selected for DNA extraction. The primers that bind to the hypervariable region V3-V4 (341F: 5'-ACTCCTACGGGAGGCAG CAG-3'; 806R: 5'-GGACTACHVGGGTWTCTAAT-3') were chosen for PCR amplification of faecal bacterial DNA samples. The amplicons were purified through the magnetic bead of Agencourt AMPure XP, and a Qubit 4 fluorometer was used for quantitation.

Enzyme-linked immunosorbent assay (ELISA)

Total protein was separated from the intestine (0.1-0.25 g) using 500 μL cold RIPA buffer. Then, the samples were subjected to ultrasonic processing. Finally, the intestinal protein was obtained by centrifugation (10,000 × g, 4 °C, 10 min). IAA and IL-22 levels in 100 μL of ileum tissue supernatant were measured using a commercial ELISA kit (Cloud-Clone, Wuhan, China).

Statistical analysis

The results are expressed as the mean ± SEM. Significant differences were analysed via one-way analysis of variance (ANOVA) and least significant difference (LSD) tests. $p<0.05$ was considered to indicate statistical significance.

Results

Isolation and identification of LA-QC1H

As shown in Fig. 1A, the purified colonies were mostly white or milky white with round, neat edges, approximately 2-3 mm in diameter, and a moist and smooth surface. Light microscopy revealed that the isolated strains were gram-positive, long rod-shaped, not arranged in chains, and existed individually (Fig. 1B).

The identity of the isolated strain was then determined using 16 S rDNA sequencing. Based on the constructed phylogenetic tree, the homology of QC1H with *Lactobacillus amylovorus* was 100%, and QC1H is a member of the *Lactobacillus* family (Fig. 1C).

Isolation and characterization of LA.EVs

LA.EVs were obtained from the culture supernatants of *Lactobacillus amylovorus* by using gradient centrifugation and ultracentrifugation (Fig. 1D). To assess the characterization of LA.EVs, transmission electron microscopy (TEM) and nanoparticle tracking analysis (NTA) analysis were used for LA.EVs samples. As shown in Fig. 1E, the TEM images revealed a closed spherical membrane structure. The sizes of the EVs ranged from 170 to 310 nm, as shown by NTA analysis in Fig. 1F. These results demonstrated that LA.EVs were extracted and obtained successfully.

LA.EVs ameliorated AFB1-induced inflammatory intestinal injury in mice

To investigate the intervention effect of LA.EVs, AFB1 and LA.EVs were administered to mice through orally gavage once daily for 28 days (Fig. 2A). The intestinal tract is a barrier to prevent pathogeny from passing into other tissues. Therefore, intestinal pathology and related gene expression analyses were performed. Figure 2B showed the body weight changes in the different groups. The average weights of the AFB1 group were always lower than the those of the control group, and the

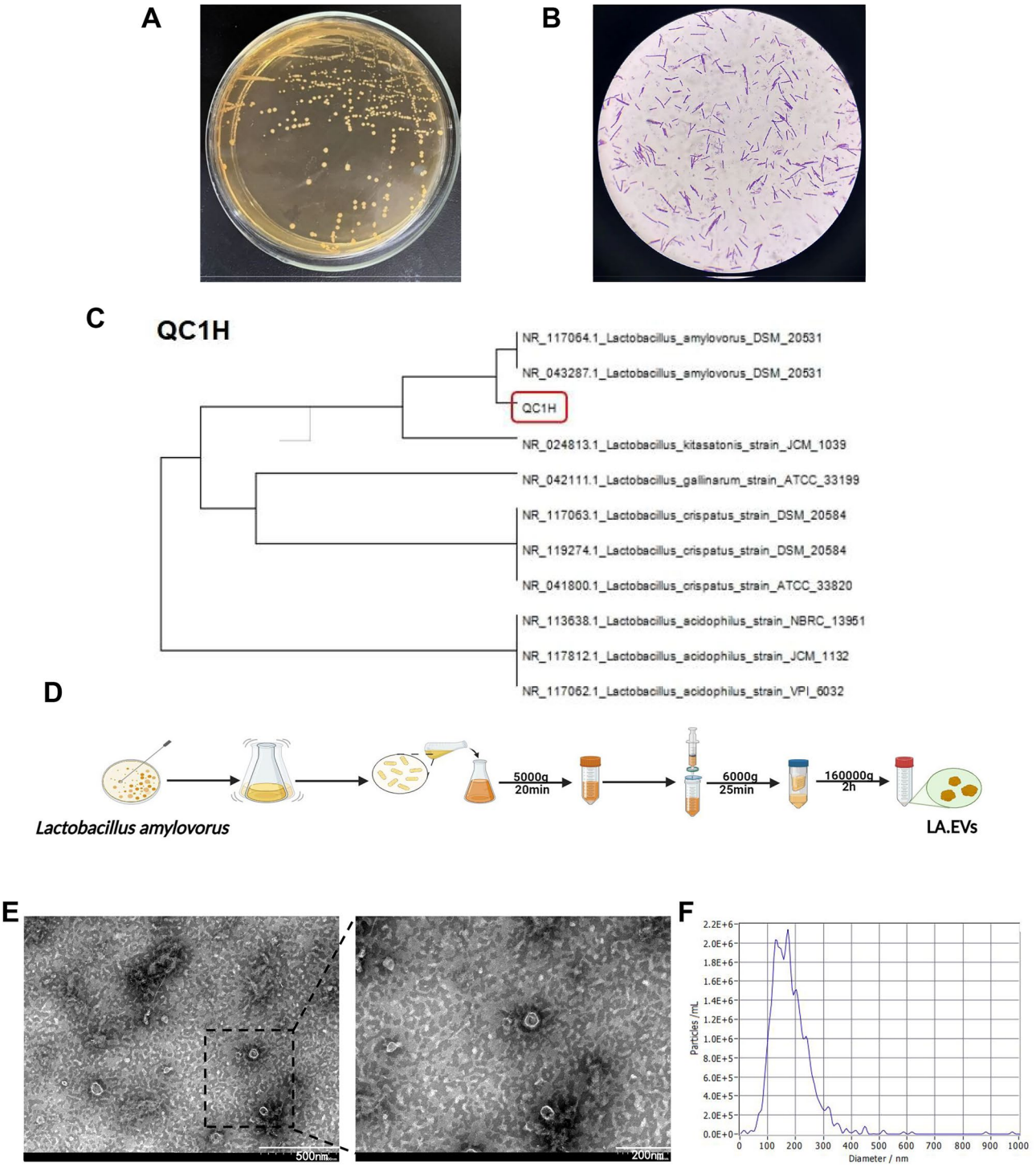

Fig. 1 Characterization of LA and LA.EVs. (**A**) Colony morphology of *Lactobacillus amylovorus-QC1H* (LA-QC1H) on MRS agar medium. (**B**) Gram staining results of LA-QC1H. (**C**) Phylogenetic tree of LA-QC1H inferred from the 16 S rDNA gene sequences. (**D**) A schematic illustration of the isolation method for LA.EVs. (**E**) Transmission electron microscopy images of isolated EVs. The scale bar is 200 nm. (**F**) The particle size of LA.EVs was measured by nanoparticle tracking analysis (NTA)

LA.EVs group showed the same increasing trend as the CON group. Figure 2C and D showed that the intestinal length was markedly shorter in the AFB1 group than in the CON group, but was significantly reversed to the normal level in the AFB1+LA.EVs group. H&E staining images of the ileum in the different groups were shown in Fig. 2E and F. The structure of the intestinal epithelium in the CON group was relatively intact, and there was no

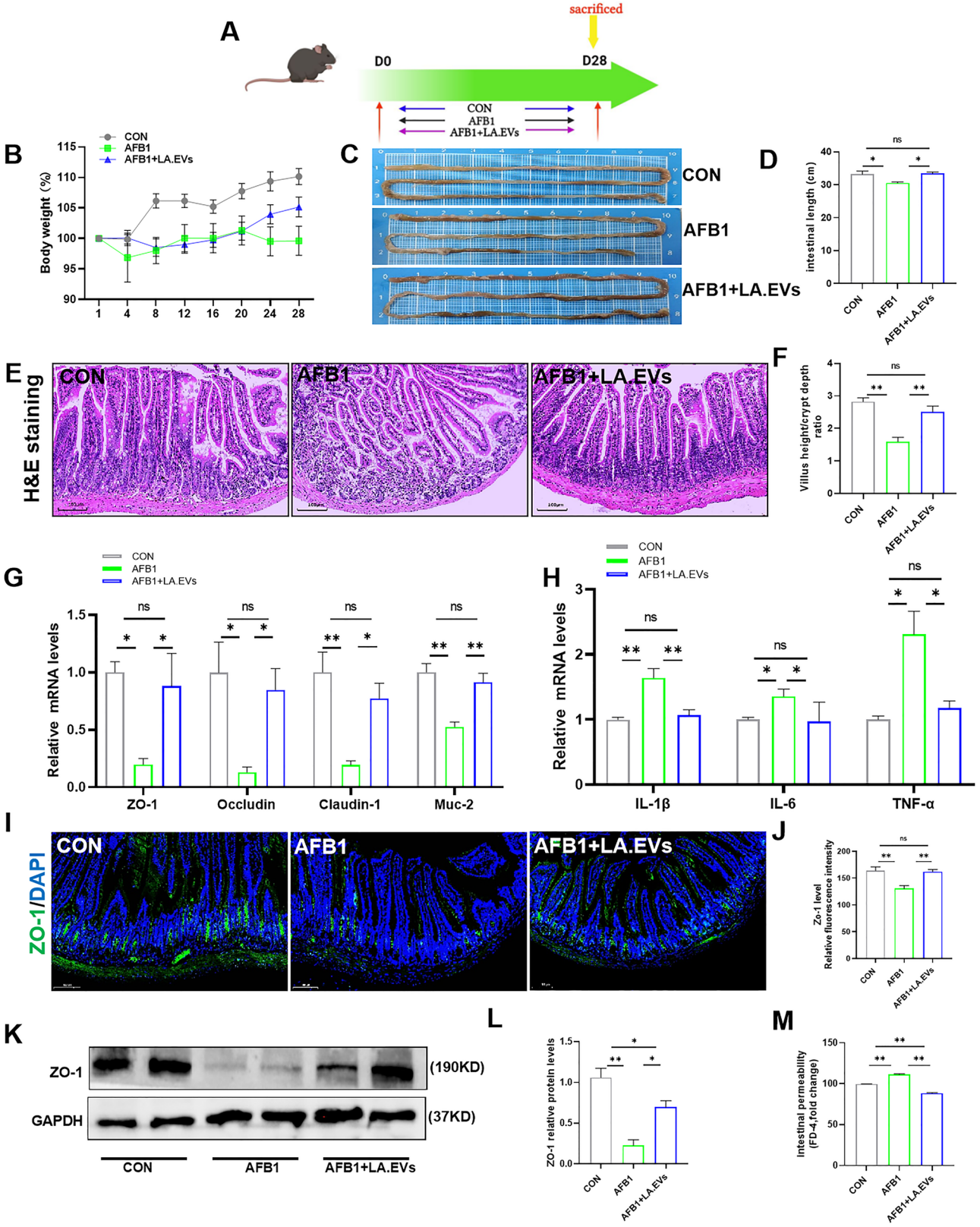

Fig. 2 (See legend on next page.)

(See figure on previous page.)

Fig. 2 Effects of LA.EVs treatment on inflammatory intestinal injury in AFB1-exposed mice. (**A**) Experimental design. (**B**) Body weight change. (**C**) Typical photos of intestines in the three groups. (**D**) Corresponding intestinal length was measured. (**E**, **F**) Representative image of H&E staining of ileum sections (scale bar = 100 μm) and statistical analysis of the villus height/crypt depth ratio. (**G**) Relative mRNA levels of tight junction proteins and muc-2 were measured in the ileum by qRT-PCR. (H) IL-1β, IL-6, and TNF-α mRNA abundances in the ileum were measured by real-time PCR analysis. (I, J) Representative immunofluorescence staining of ZO-1 antibody in the ileum (scale bar = 100 μm). (K, L) Relative protein abundances of ZO-1 in the intestine. (M) Intestinal permeability was measured by serum FD-4 concentration ($n = 5$). Values are expressed as the mean ± SEM. *$p < 0.05$, **$p < 0.01$, ns, the difference is not significant

obvious inflammation. However, in the AFB1 group, the structure of the intestinal epithelium was incomplete, and the intestinal villi were disrupted. Compared to the AFB1 group, the AFB1+LA.EVs group had complete and longer intestinal villi and shallower crypt depth. In addition, the ratio of villus height to crypt depth was not significant different between the LA.EVs group and CON group. The observations of intestinal length and H&E staining indicated that AFB1 caused intestinal injury and LA.EVs could improve intestinal morphology damaged by AFB1. Altered tight junctions can weaken barrier function and epithelial integrity. Compared with those in the CON group, the mRNA expression levels of tight junction proteins (ZO-1, Occludin and Claudin-1) and mucus were significantly lower in the AFB1 group. Conversely, the mRNA expression of tight junction proteins was markedly increased by the LA.EVs treatment, and the levels were not significantly differ from those in the CON group(Fig. 2G). The LA.EVs treatment also alleviated the AFB1-induced inflammation, and the results of intestinal proinflammatory cytokine (IL-1β, IL-6 and TNF-α) secretion are shown in Fig. 2H. The results showed that the mRNA expression of proinflammatory cytokines was significantly increased in the AFB1 group compared to the CON group, and markedly reversed to the level of CON group in LA.EVs group. In addition, a high serum fluorescence intensity of FD-4 indicates increased intestinal permeability. We found that the level of FD-4 in the AFB1 group was significantly greater than that in the CON group, and these changes were markedly reversed in the LA.EVs group (Fig. 2M). And the level of FD-4 in the AFB1+LA.EVs group was lower than that in the CON group. The results of immunofluorescence staining (Fig. 2I and J) and protein expression of ZO-1 (Fig. 2K and L) showed that LA.EVs treatment markedly alleviated the decrease in ZO-1 in the AFB1 group, and the level of ZO-1 of the AFB1+LA.EVs group was significantly decreased compared to the CON group. Thus, the above results suggested that LA.EVs had a protective function in alleviating AFB1-induced intestinal injury in mice.

LA.EVs altered the diversity and composition of the gut microbiota in AFB1-exposed mice

To investigate the changes in the gut microbiota composition, we performed 16 S rRNA gene sequencing on the faecal samples of the mice. Alpha diversity was assessed according to the Shannon and Simpson indices, as shown in Fig. 3A and B. The results of Shannon index (Fig. 3A) showed that AFB1 mice had markedly decreased microbial community diversity than the CON mice, and AFB1+LA.EVs mice had an increased tend compared to the AFB1 mice. The Simpson index value is negatively correlated with the alpha diversity. The Simpson index (Fig. 3B) revealed that there was a lower community diversity in AFB1 mice than that in CON mice, and AFB1+LA.EVs mice had higher community diversity than that in AFB1 mice. But there were no differences in alpha diversity were detected. Beta diversity was measured using principal coordinates analysis (PCoA) (Fig. 3C) and non-metric multidimensional scaling (NMDS) (Fig. 3D), to identify differences in gut microbiota composition among the three groups. The results revealed that each group clustered separately, suggesting that both treatment (AFB1 and AFB1+LA.EVs) changed the compositions of the gut microbiota. The evolutionary branching tree (Fig. S1A) also showed the diversity of species abundance. In addition, we compared the gut microbiota variations at different classification levels. At the phylum level, *Bacteroidetes* and *Firmicutes* were the most dominant taxa (Fig. 3E). The relative abundance of *Bacteroidetes* was markedly lower in the AFB1 group than in the CON group, but the relative abundance of *Firmicutes* was significantly increased. The LA.EVs treatment had a significantly increased relative abundance of *Bacteroidetes*, and there was no significant difference of *Bacteroidetes* in the control group (Fig. 3F). LA.EVs treatment markedly decreased relative abundance of *Firmicutes*, and the abundances of *Firmicutes* was significantly decreased in the AFB1+LA.EVs group compared with the CON group (Fig. 3G). Moreover, the *Firmicutes/Bacteroidetes* ratio in the AFB1 group was significantly greater than that in the CON group, while the LA.EVs treatment markedly reversed these effects. And this ratio was lower in the AFB1+LA.EVs group than that in the CON group (Fig. 3H). At the order level, the enriched taxa primarily included *Bacteroidales and Clostridiales* (Fig. 3I). The relative abundance of *Bacteroidales* decreased significantly in the AFB1 group. Interestingly, the LA.EVs treatment significantly reversed these changes to the same extent as those in the CON group (Fig. 3J). However, there was no significant difference in *Clostridiales* abundance among the three groups (Fig. 3K). At the genus level, a heatmap revealed

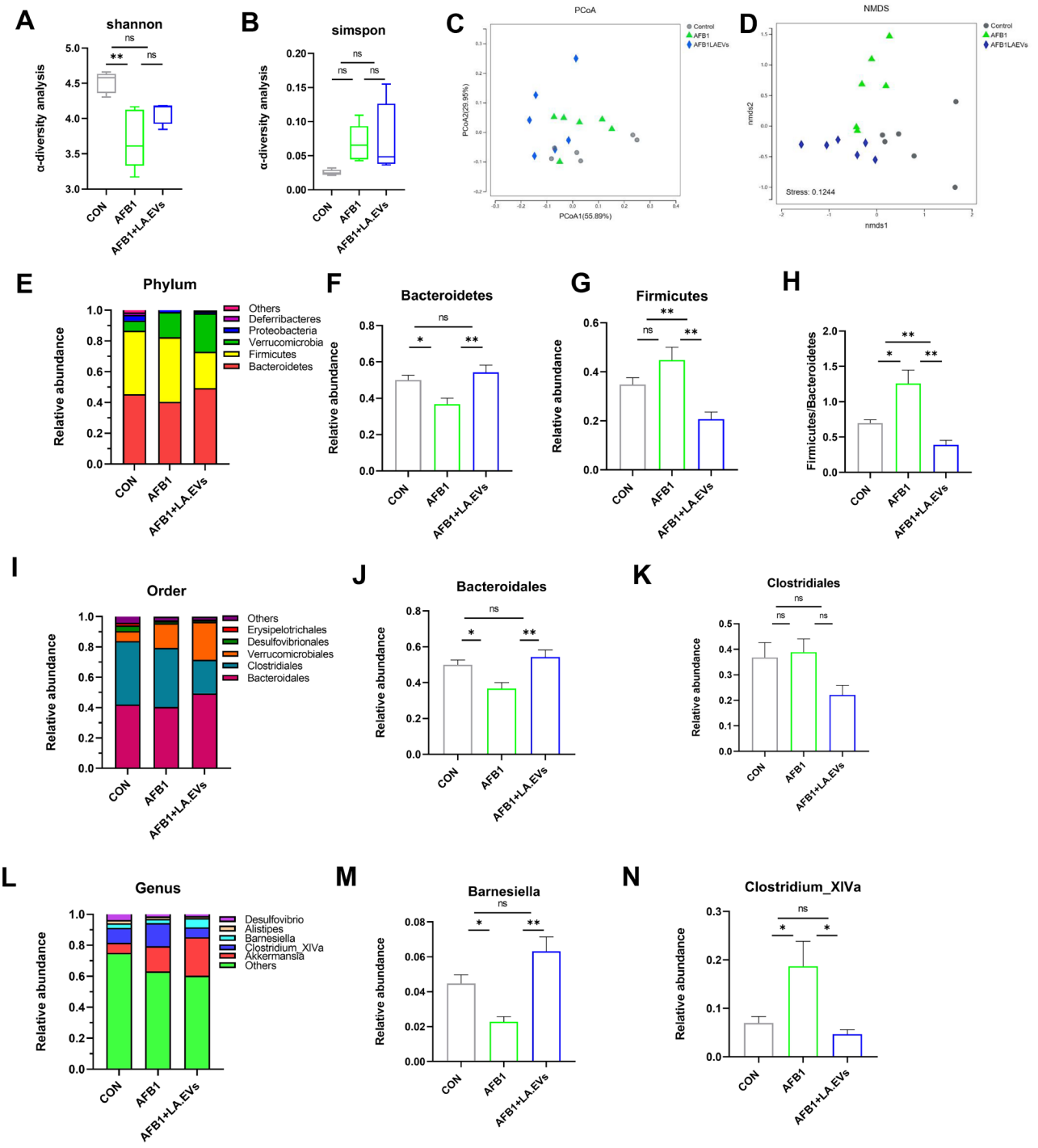

Fig. 3 Effects of LA.EVs treatment of the intestinal microbiota in AFB1-exposed mice. (**A**, **B**) Shannon and Simpson indices in α-diversity analysis. (**C**, **D**) Beta diversity was assessed by PCoA and NMDS analysis for each group. (**E**-**H**) Microbiota compositions at the phylum level. (**I**-**K**) Microbiota compositions at the order level. (**L**-**N**) Microbiota compositions at the genus level ($n = 5$). Values are expressed as the mean ± SEM. *$p < 0.05$, **$p < 0.01$, ns, the difference is not significant

the species composition (Fig. S2A), and the increase in *Bacteroides* abundance was reversed in the AFB1+LA.EVs group (Fig. S1B). At the genus level, the enriched taxa primarily included *Barnesiella and Clostridium_XlVa* (Fig. 3L). The relative abundance of *Barnesiella*, significantly decreased in AFB1-exposed mice, but markedly increased and returned to the CON level in the LA.EVs group (Fig. 3M). In addition, the abundance of *Clostridium_XlVa* significantly increased in AFB1-exposed mice, but markedly decreased in AFB1+LA.EVs

mice (Fig. 3N). And there was no significant difference in the abundance of *Clostridium_XIVa*. between the LA.EVs group and CON group. To explore the functional impacts of the gut microbiota compositions among the three groups, we performed Kyoto Encyclopedia of Genes and Genomes (KEGG) pathway and Clusters of Orthologous Groups of Proteins (COG) analyses. KEGG analysis (Fig. S3A and B) revealed that many bacteria were involved in carbohydrate, amino acid, cofactor and vitamin metabolism. The COG data (Fig. S4A and B) revealed that many bacteria were involved in translation, ribosomal structure and vitamins, amino acid transport and metabolism, carbohydrate transport and metabolism. In summary, these findings suggested that AFB1-induced intestinal microbiota dysbiosis was effectively reversed by LA.EVs treatments to a certain extent.

LA.EVs activated intestinal AHR/IL-22 signalling in AFB1-exposed mice

Previous research had shown that *Barnsiella* mainly played a role in tryptophan metabolism, and produce indole and its derivatives, then activate AHR and further encourage intestinal homeostasis by inducing IL-22 [33]. Combined with the changes in the abundance of *Barnsiella* in the 16 S rRNA results and the pathway prediction results, we can conclude that the activation of AHR signaling pathway may be a potential mechanism for LA.EVs to alleviate intestinal injury induced by AFB1. To further investigate the mechanism by which LA.EVs exerted protective effects on AFB1-exposed mice, the levels of IAA, endogenous ligand of AHR, were determined. Our study showed that the intestinal IAA level of LA.EVs treatment was markedly increased compared to those of the AFB1-exposed mice, and there was no significant difference compared to the CON group (Fig. 4A). As IAA is an endogenous ligand of the AHR receptor, we analyze the expression of AHR. Moreover, the mRNA expression levels of cytochrome P450 family 1 subfamily A member 1 (CYP1A1) and IL-22, which are two transcriptional targets of AHR, were analyze. The results showed that AHR, CYP1A1, and IL-22 gene expressions were markedly decreased in AFB1-exposed mice, but significantly increased in the LA.EVs group compared to AFB1group (Fig. 4B-D). The mRNA expression of AHR and IL-22 in the LA.EVs group were not significantly different from that in the CON group. But the mRNA expression of CYP1A1 in the AFB1+LA.EVs group was significantly decreased compared to the CON group. Reg3g and Reg3b, antimicrobial peptide secreted by IL-22, can effectively resist the invasion of external pathogens. The results showed that the mRNA expression levels of Reg3g and Reg3b in the AFB1 group were significantly lower than those in the CON group, while were significantly upregulated in the LA.EVs group (Fig. 4E and F). Meanwhile, the LA.EVs treatment markedly increased the protein level of intestinal IL-22 in AFB1-exposed mice (Fig. 4G). As shown in Fig. 4H and I, the distribution of intestinal AHR protein was significantly decreased after AFB1 treatment, but was markedly increased in the AFB1+LA.EVs group. And compared with the CON group, the distribution of intestinal AHR protein was significantly decreased in the AFB1+LA.EVs group. Moreover, intestinal AHR protein expression was measured by Western blotting. Figure 4J and K showed that AHR protein expression was significantly decreased in the AFB1 group. However, compared with that in the AFB1 group, AHR protein expression was significantly increased in the LA.EVs group, and there was no significant difference between the LA.EVs group and CON group. These findings suggested that AHR/IL-22 signalling may be the potential mechanism for LA.EVs prevented AFB1-induced inflammatory intestinal injury.

LA.EVs failed to relieve AFB1-induced inflammatory intestinal injury in antibiotic-treated mice

To further evaluate the role of the gut microbiota in the alleviation of intestinal injury by LA.EVs in AFB1-exposed mice, depleted the gut microbiota by using an ABX blend (Fig. 5A). Oral gavage antibiotic solution for seven days and fecal coating were performed to confirm that all gut microbes had been removed, and drinking the mixed antibiotic solution throughout the experiment was used to maintain the absence of gut microbiota. Compared to the AFB1+LA.EVs treated mice, the AFB1+LA.EVs+ABX mice showed shorter intestinal villi and deeper crypt depths (Fig. 5B and C). In addition, the ileum ZO-1 protein level in the AFB1+LA.EVs+ABX group was significantly decreased compared to AFB1+LA.EVs group, which was subjected to immunofluorescence analysis (Fig. 5B and D). The content of serum FD-4 in AFB1+LA.EVs+ABX group mice was higher than that in AFB1+LA.EVs group mice (Fig. 5E), indicating that antibiotic treatment significantly increased intestinal permeability. Moreover, compared to AFB1+LA.EVs-treated mice, antibiotic-treated mice had lower mRNA expression levels of ileum tight junction proteins and muc-2 (Fig. 5F). The ileum mRNA expression levels of proinflammatory cytokines were significantly increased in the AFB1+LA.EVs+ABX group compared with the AFB1+LA.EVs group (Fig. 5G). According to the previous results, it was found that LA.EVs could alleviate the intestinal damage caused by AFB1 exposure in normal mice. Interestingly, the effect of LA.EVs on the intestinal damage caused by AFB1 disappeared after clearance of gut microbiota. These results showed that LA.EVs exerted protective effects on AFB1-induced inflammatory intestinal injury through the gut microbiota. However, the use of a mixture of antibiotics will clear all the

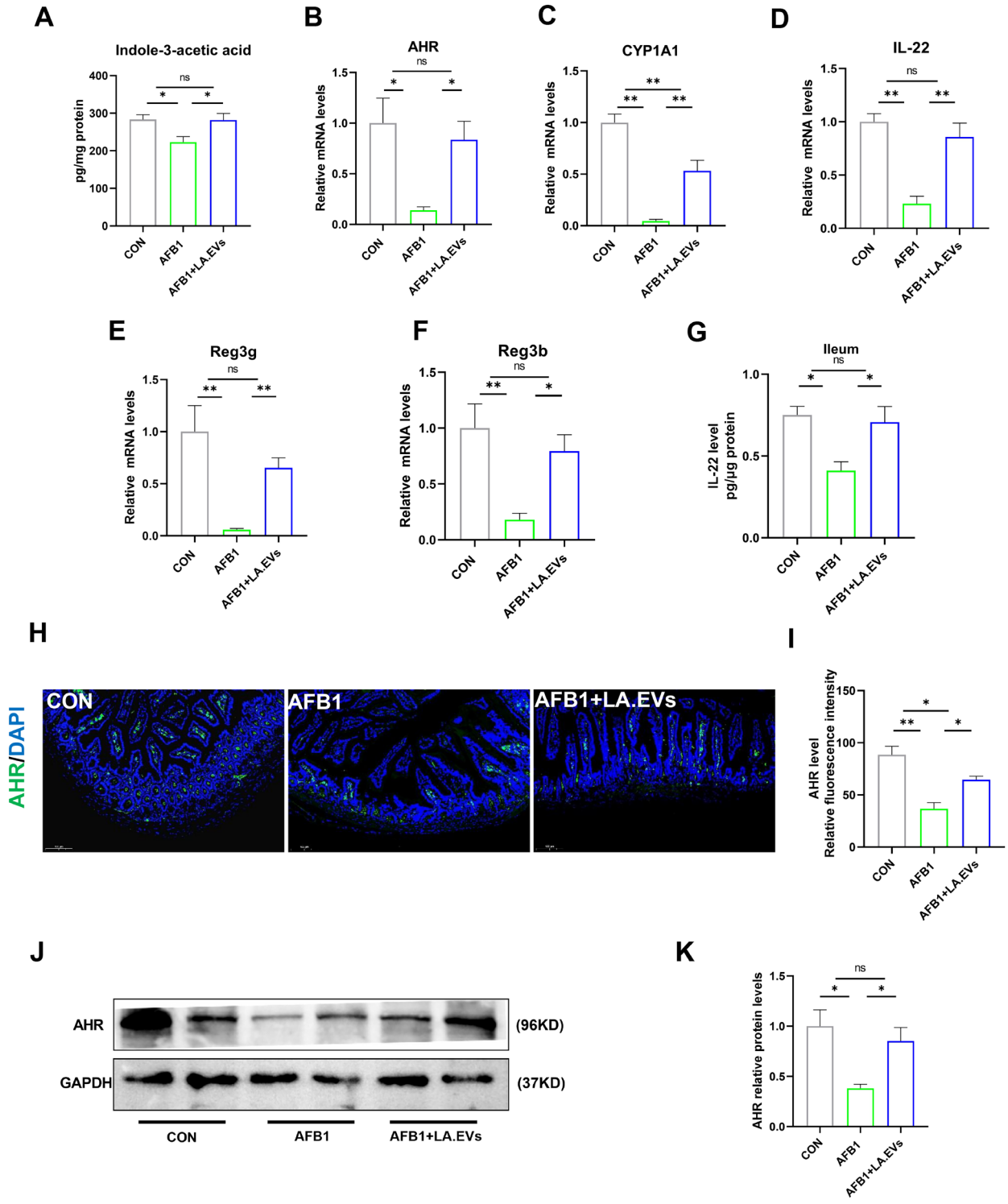

Fig. 4 Effects of LA.EVs treatment of the ileum AHR/IL-22 axis in AFB1-exposed mice. (**A**) The ileum IAA levels were measured by ELISA. (**B**-**F**) Relative mRNA levels of AHR, CYP1A1, IL-22, Reg3g and Reg3b were measured in the ileum by qRT-PCR. (**G**) Ileum IL-22 levels were measured by ELISA. (**H**, **I**) Image of AHR IF staining in the ileum (scale bar = 100 μm). (**J**, **K**) Relative protein abundances of AHR in the intestine ($n = 5$). Values are expressed as the mean ± SEM. *$p < 0.05$, **$p < 0.01$, ns, the difference is not significant

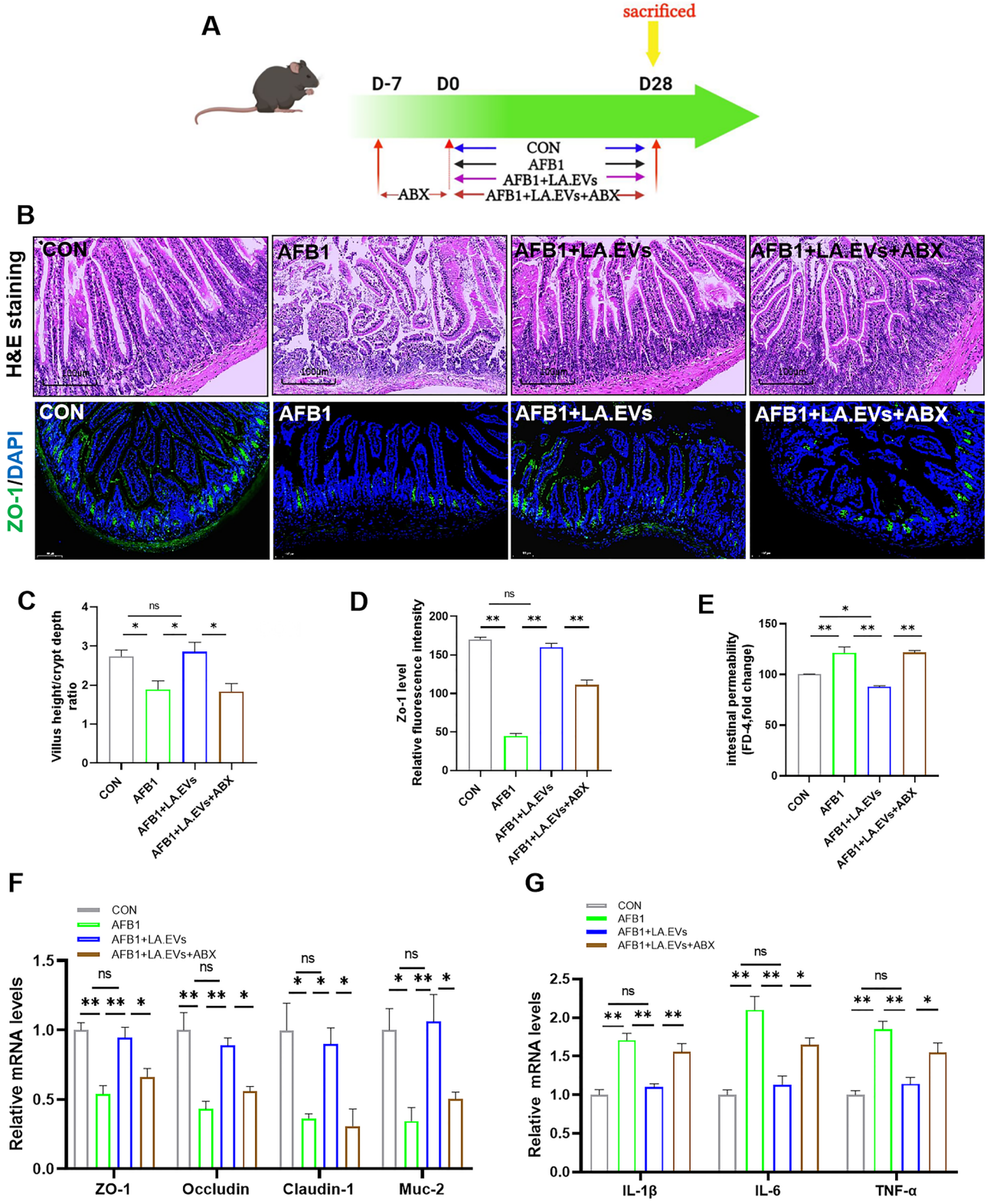

Fig. 5 Effects of LA.EVs treatment on AFB1-induced intestinal injury in ABX mice. (**A**) Experimental design. (**B**) Representative image of H&E and ZO-1 antibody immunofluorescence staining of the ileum (scale bar = 100 μm). (**C**) Statistical analysis of the villus height/crypt depth ratio. (**D**) Statistical analysis of relative fluorescence intensity. (**E**) Intestinal permeability was assessed by serum FD-4 concentration. (**F**) Tight junction proteins and muc-2 mRNA abundances in the ileum were measured by qRT-PCR analysis, and relative gene expression was normalized to GAPDH. (**G**) Relative mRNA levels of proinflammatory factors were measured in the ileum by qRT–PCR ($n = 5$). Values are expressed as the mean ± SEM. *$p < 0.05$, **$p < 0.01$, ns, the difference is not significant

gut microbiota in the intestine, and further studies are needed to investigate which specific microbiota changes play a major role in alleviating the intestinal injury induced by AFB1.

LA.EVs failed to activate intestinal AHR/IL-22 signalling in antibiotic treated mice

To determine the mechanism of gut microbiota in the protective effects of LA.EVs, AHR/IL-22 signalling is also verified. Compared with AFB1+LA.EVs group, the expressions of AHR signalling pathway-related genes (AHR, IL-22, and CYP1A1) (Fig. 6A-C) and protein (AHR) (Fig. 6G and H) in the intestine were significantly decreased in antibiotic-treated mice. The elimination of the gut microbiota also weakened the protective effect of LA.EVs, as Reg3g and Reg3b mRNA expression decreased (Fig. 6D and E). Moreover, Fig. 6F showed that the ileum IL-22 protein level in antibiotic-treated mice was significantly lower than that in AFB1+LA.EVs-treated mice. These results suggested that LA.EVs exerted a protective effect on AFB1-induced inflammatory intestinal injury through intestinal microbiota-mediated AHR/IL-22 signalling.

LA.EVs ameliorated AFB1-induced inflammatory intestinal injury by activating intestinal AHR/IL-22 signalling in mice

To further examine whether the protective effects of LA.EVs on intestinal injury are activated by intestinal AHR signalling, we treated AFB1-exposed mice with the AHR antagonist CH223191 (Fig. 7A). As shown in Fig. S5A-E, CH223191 treatment significantly decreased the mRNA expression levels of AHR, CYP1A1, IL-22, Reg3g and Reg3b in the AFB1+LA.EVs mice. Moreover, the ileum protein level of IL-22 was significantly decreased in the AFB1+LA.EVs+CH group compared with the AFB1+LA.EVs group (Fig. S5 F). The ileum AHR protein distribution in the AFB1+LA.EVs+CH group was decreased compared to that in the AFB1+LA.EVs group (Fig. S5G and H). These results indicated that AHR signalling was significantly inhibited. After ensuring that AHR signal was suppressed, intestinal pathological changes and intestinal damage were evaluated in the CH223191 group of mice. H&E-stained images of the AFB1+LA.EVs+CH group indicated that the ileum structure was severely destroyed compared to that of the AFB1+LA.EVs group (Fig. 7B and C). Figure 7B and D showed that the ileum ZO-1 protein abundance in CH223191-treated mice was significantly decreased. Moreover, CH223191 treatment significantly increased intestinal permeability, as indicated by the fluorescence intensity of FD-4 (Fig. 7E). The mRNA expression of tight junction proteins and muc-2 in the AFB1+LA.EVs+CH group was decreased compared to that in the AFB1+LA.EVs group (Fig. 7F). As shown in Fig. 7G, the mRNA expression levels of IL-1β, IL-6, and TNF-α were significantly increased in the AFB1+LA.EVs+CH group compared to the AFB1+LA.EVs group. Taken together, these results confirmed that the protective effects of LA.EVs on AFB1-induced inflammatory intestinal injury by the activation of intestinal AHR/IL-22 signalling. However, the role of AHR cannot be fully demonstrated with just one AHR inhibitor. Inhibitors with various characteristics and intestinal-specific AHR knockout mice model were needed to further confirm the requirement of AHR in the action of LA.EVs in intestinal damage induced by AFB1.

Discussion

Aflatoxin contamination has become a widespread and unavoidable public health concern [34], and AFB1-induced hepatotoxicity has attracted considerable attention [35]. However, excessive intake or susceptibility to AFB1 exposure can occur in tissues other than the liver. The intestinal tract, which is the first barrier to aflatoxin exposure, is likely a target organ for AFB1. Previous research have shown that AFB1 can be metabolized into toxic metabolites through cytochromes P450 enzymes in the digestive tract, therefore, AFB1-induced intestinal injury cannot be ignored [36]. Some studies have revealed that AFB1 exposure decreased the expression of tight junction proteins and caused intestinal inflammation in vivo [37–39]. In addition, AFB1 inhibits cell viability and the expression of intestinal tight junction proteins in vitro [40, 41]. In this study, we found that AFB1 exposure induced intestinal injury by reducing the body weight, length, and villus height/crypt ratio of the ileum in mice. Moreover, AFB1 exposure increased the secretion of proinflammatory cytokines and enhanced intestinal permeability.

EVs, a kind of membrane vesicle secreted by most living organisms on earth, play a critical role in bacteria-host interactions [42]. EVs carry a wide variety of bioactive materials including proteins, lipids, polysaccharides and RNAs, and are believed to influence bacterial and host cell functions, thereby influencing host metabolism and the immune response. Recent studies have also revealed that EVs secreted by bacteria played an important role in the interaction between the host and the human microbiome [43]. Bacteria-derived EVs have been used as effective tools for drug delivery and disease diagnosis due to their low cost and ease of isolation and manipulation [44]. *Lactobacillus amylovorus* is a primary species of *Lactobacillus* in the small intestine of mammals, including pigs, rats, and rhesus macaques [45, 46]. Emerging evidence have revealed the beneficial effect of *L. amylovorus* SLZX20-1 both in vitro and in vivo. *L. amylovorus* SLZX20-1 markedly activated the expression of host defence peptides (HDPs) in IPEC-J2 cells. Moreover, it significantly improved the jejunum and

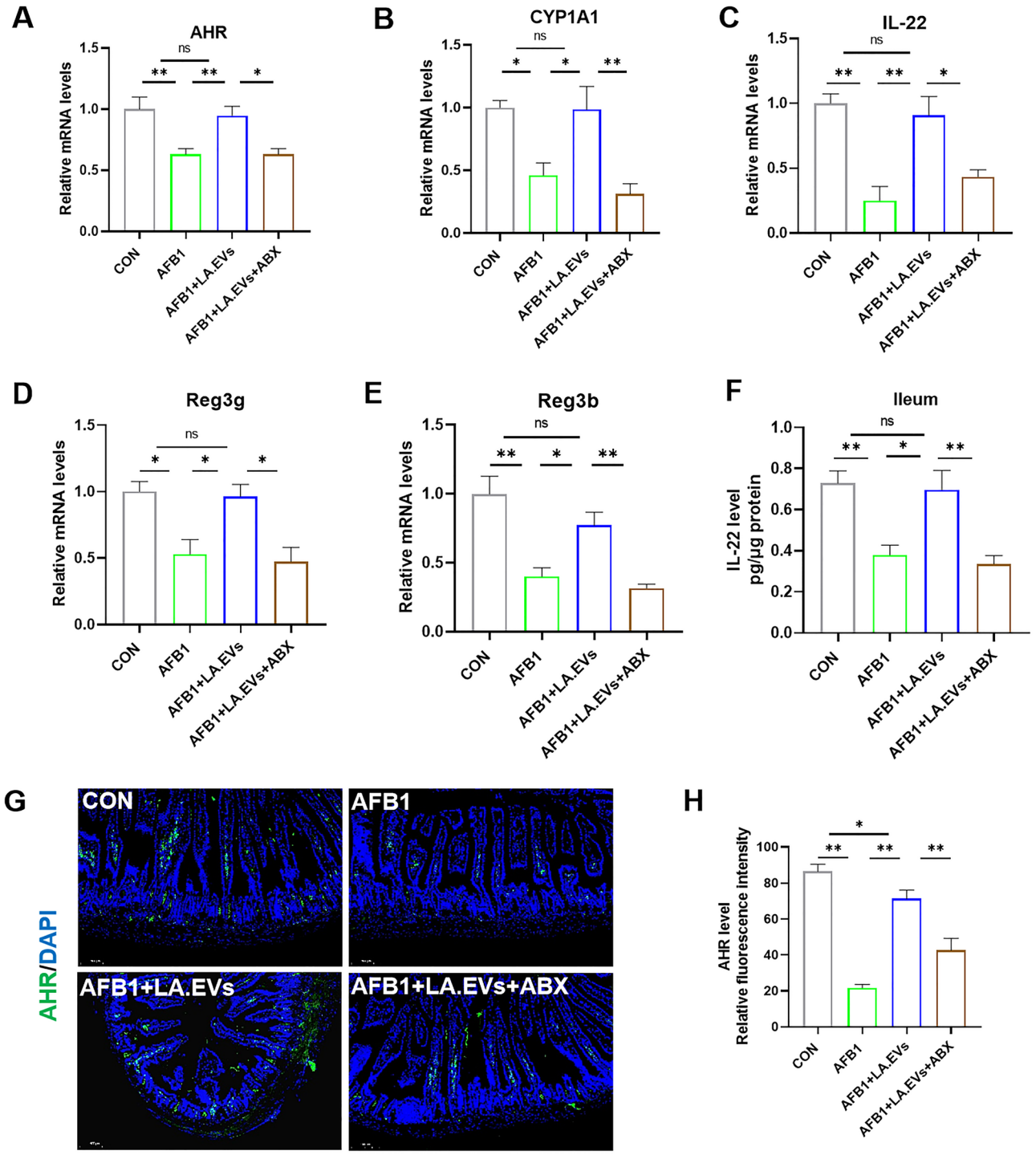

Fig. 6 Effects of LA.EVs treatment of the ileum AHR/IL-22 signalling in antibiotic-treated mice. (**A**-**E**) AHR, CYP1A1, IL-22, Reg3g and Reg3b mRNA abundances in the intestine were measured by real-time PCR analysis. (**F**) Ileum IL-22 levels were measured by ELISA. (**G**, **H**) Representative image of AHR IF staining in the ileum (scale bar = 100 μm) ($n = 5$). Values are expressed as the mean ± SEM. *$p < 0.05$, **$p < 0.01$, ns, the difference is not significant

ileum and changed the composition of gut microbes in mice [47]. Liang et al. reported that *C. butyricum*-derived EVs administration could alleviate colon inflammation [16]. However, whether LA.EVs treatment can ameliorate AFB1-induced intestinal injury remains unknown. In this study, we extracted and obtained LA.EVs from the culture supernatants of LA, and TEM images showed a bilayered, closed and nanosized membrane structure. Additionally, we observed that LA.EVs had protective effects on AFB1-induced inflammatory intestinal injury.

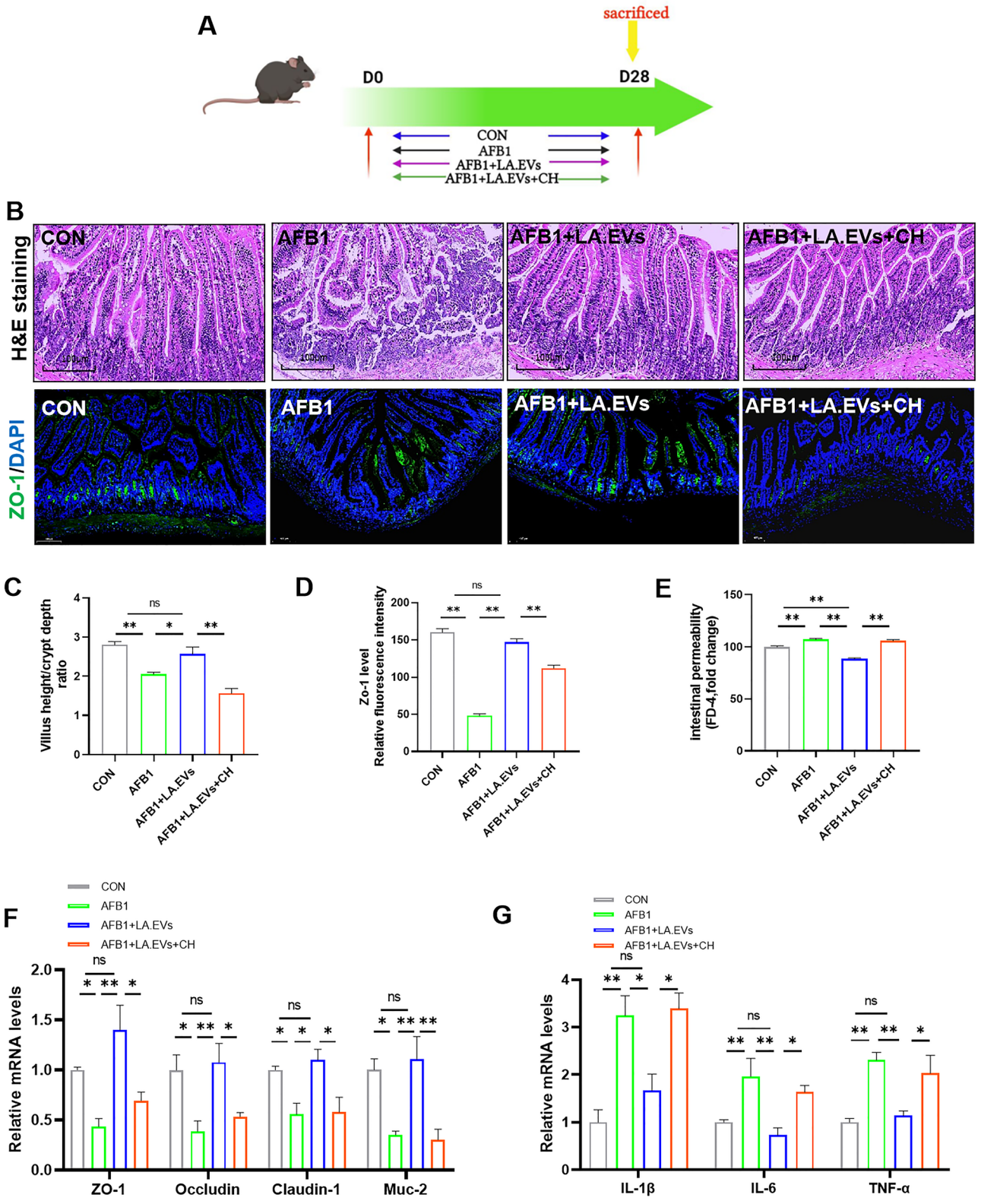

Fig. 7 Inhibition of intestinal AHR activation abolished the protective effects of LA.EVs. (**A**) Experimental design. (**B**) Representative image of H&E and ZO-1 antibody IF staining of ileum sections (scale bar = 100 μm). (**C**) Statistical analysis of the villus height/crypt depth ratio. (**D**) Statistical analysis of relative fluorescence intensity. (**E**) Intestinal permeability was assessed by serum FD-4 concentration. (**F**) Tight junction proteins and muc-2 mRNA abundances in the ileum were measured by real-time PCR analysis. (**G**) Relative mRNA expression levels of IL-1β, IL-6 and TNF-α were measured in the ileum by qRT-PCR ($n = 5$). Values are expressed as the mean ± SEM. *$p < 0.05$, **$p < 0.01$, ns, the difference is not significant

However, due to the limitations of extracellular vesicles stability and storage conditions, further explorations are needed to optimize the use of LA.EVs.

The gastrointestinal tract is the largest surface of the body exposed to the exoteric environment, it performs food digestion and acts as a key line of defence. Many diseases are accompanied by intestinal damage, including inflammatory bowel diseases, chronic liver diseases, cardiovascular diseases and chronic kidney disease [48]. Intestinal tract is a barrier to prevent harmful substances from passing into other tissues. The invasion of external pathogens can damage and shorten the intestines. AFB1 exposure can affect intestinal nutrient absorption, damage intestinal morphology and intestinal barrier integrity [49, 50]. Moreover, it has been found that inflammatory infiltration can shorten the length of the intestine [51]. In our study, we showed that AFB1 exposure could induced weight loss, increased intestinal inflammatory factors, and decreased intestinal barrier function in mice. The intestinal barrier is an important line of defence that maintains the homeostasis of intestinal microenvironments [52]. The epithelial cell layer is the core of the intestinal barrier. Intestinal epithelial cells are tightly connected through a cross complex composed of tight junctions, adherence junctions and basolateral desmosomes [53]. Disruption of the gut barrier has been correlated with a decrease in the production of mucus and antimicrobial peptides and a decrease in tight junctions [54]. Research has shown that AFB1 can destroy the intestines of livestock and poultry by polluting their food and eventually affecting the function [55]. Our study also revealed that AFB1 exposure caused intestinal injury by decreasing the mRNA and protein expression of tight junction proteins and muc-2 (Fig. 2). Interestingly, it have been reported that *L. amylovorus* DSM 16698T and its cell-free supernatant can alleviate ETEC K88-induced intestinal injury by inhibiting TLR4 signalling [12]. Our study demonstrated the protective effect of LA.EVs in AFB1-induced intestinal injury. The results showed that the LA.EVs treatment alleviated AFB1-induced intestinal injury by decreasing intestinal permeability and the mRNA expression of inflammatory cytokines, and increasing the expression of tight junction proteins.

Previous research has shown that normal faeces can effectively restore the intestinal barrier and rescue colitis through recovering the intestinal microbiota [18]. The gut microbiota plays a vital role in host food metabolism, nutrient absorption, and mucosal barrier integrity [56]. However, whether the protective effects of LA.EVs on AFB1-induced intestinal injury are connected to the gut microbiota is unclear. In 16 S rRNA gene sequencing, α-diversity refers to the diversity within a specific region or ecosystem and is a comprehensive indicator of richness and evenness. The β-diversity refers to the species diversity between different environmental communities. The β-diversity, together with α-diversity, constitutes the overall diversity or the biological heterogeneity of a given environmental community [57]. In our study, we explored species similarity or differences of microbial communities in beta diversity, including PCoA and NMDS. The result showed that the samples of CON group and AFB1 group were obviously separated, which indicated that the gut microbiota of CON and AFB1group had obvious variation. After the treatment of LA.EVs, the distribution of gut microbiota tended to migrate to the CON group. Although there was no significant difference in α-diversity, there was a significant difference in β-diversity. The above results can still indicate that LA.EVs had a certain regulatory effect on the composition of gut microbiota community in AFB1 mice. Our study revealed that the composition of the gut microbiota changed and that the *Firmicutes/Bacteroidetes* ratio decreased in the LA.EVs group compared to the AFB1 group. Consistent with our findings, some studies have reported that AFB1 exposure increases the ratio and induces oxidative stress and inflammation [58, 59]. However, after EV administration, we found that the abundance of *Verrucomicrobia* (Fig. 3E and I) and *Akkermansia* (Fig. 3L), was even more from the control group. Previous research had reported that *Akkermansia muciniphila* (Akk) alleviated *C. rodentium* induced-colitis through upregulating the expressions of Reg3γ and IL-22 to enhanced mucus barrier and anti-microbial responses [60]. Akk contributes to the repair of intestinal barrier. Akk is a member of *Verrucomicrobia*, which is considered the "next generation of probiotics" [61]. In our study, Akk was increased in both the AFB1 group and AFB1+LA.EVs group, but there was no significant difference between the AFB1 group and the CON group. The reason for the increase of Akk in AFB1 group may be in response to resist the intestinal injury caused by exogenous AFB1 stimulation. Furthermore, we established an antibiotic treatment group to the role of the microbiota in the process by which LA.EVs alleviated AFB1-induced inflammatory intestinal injury. The results showed that the protective effects of LA.EVs against AFB1-induced intestinal injury were eliminated in antibiotic-treated mice. Therefore, we demonstrated that LA.EVs modulated the gut microbiota to alleviate AFB1-induced intestinal injury.

Based on the analysis of 16 S rRNA results, obvious changes can be observed in *Bacteroides spp*. The dysbiosis of the intestinal microbiota could influence the production of indole through dietary tryptophan [62]. *Bacteroides spp.* is the major producer of indole [33], As the endogenous AHR ligands, indole and its derivatives could enhance intestinal epithelial barrier functions by increasing the expression of genes involved in the

maintenance of epithelial cell structure and function [26, 63, 64].

Intestinal health is regulated by many metabolic nuclear receptors that are extensively expressed in the intestine [65, 66]. AHR activation have been shown to improve inflammatory bowel disease [67] and metabolic syndrome [68]. Specifically, AHR signalling can alleviate the function of the intestinal barrier by increasing the expression of IL-22 [29, 69] and antimicrobial proteins. Moreover, IL-22 can repair and reconstruct the intestinal barrier by improving the expression of intestinal tight junction proteins, antimicrobial peptides and mucin [27]. A previous study shows that *Lactobacillus spp*. can regulate IL-22 mucosal homeostasis via indole aldehyde-mediated activation of AHR, eventually protecting mice against mucosal candidiasis [69]. These results suggested that AHR activation is an effective method for maintaining mucosal homeostasis.

Consistently, our study revealed that LA.EVs protect against AFB1-induced intestinal injury by restoring the gut microbiota and metabolites. The low mRNA expression of AHR, CYP1A1, and IL-22 in AFB1-exposed mice, was identical to the mRNA expression of the produced mucus and antimicrobial peptides (Reg3g and Reg3b). Conversely, the expression of these genes and protein significantly increased in the LA.EVs group.

Subsequently, we sought to clarify whether the beneficial effects of LA.EVs on AFB1-induced intestinal injury were mediated by the intestinal AHR pathway. The AHR inhibitor, CH223191, was used to treat AFB1+LA.EVs mice. Interestingly, the level of intestinal inflammatory cytokines was markedly increased, as well as intestinal permeability, and the mRNA and protein expression of tight junction proteins and mucus were significantly decreased in the CH group compared with the AFB1+LA.EVs group. The above results indicated that the protective effects of LA.EVs on intestinal injury were weakened in the CH group. On this basis, we found that LA.EVs alleviated AFB1-induced intestinal injury by activating the intestinal AHR signalling. Our study provides a theoretical basis for the use of LA.EVs in the treatment of mycotoxin contamination.

Conclusions

Taken together, our study showed that LA.EVs alleviated AFB1-induced intestinal injury by modulating the gut microbiota, increasing the level of 3-IAA and activating the intestinal AHR/IL-22 signalling, thereby reducing the inflammatory response and promoting intestinal barrier repair in mice (Fig. 8). Our study further demonstrated that the potential of LA.EVs in AFB1-induced intestinal injury, providing an innovative solution for AFB1 exposure. These observations laid a solid foundation for future clinical applications of LA.EVs. However, the challenges such as weak stability and limited biosecurity faced by LA.EVs in practical applications still need to be overcome.

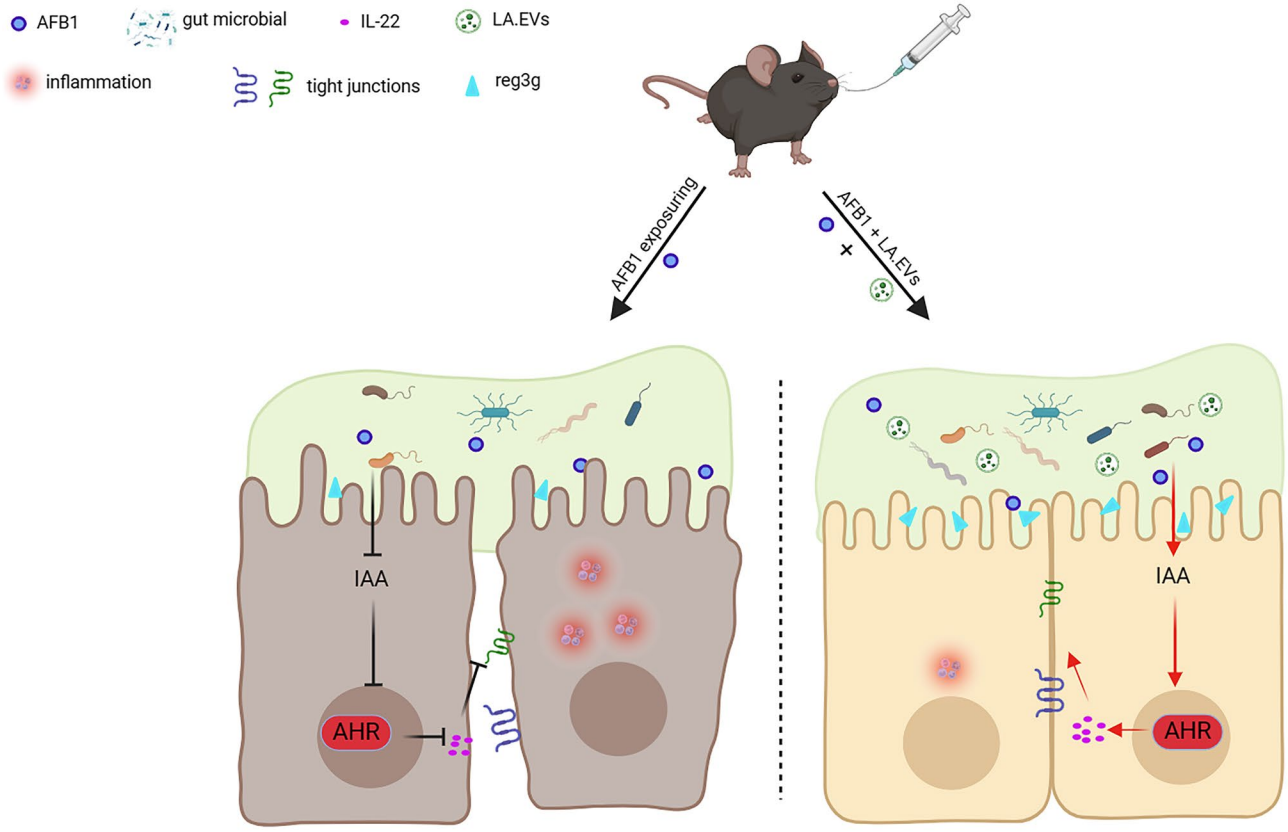

Fig. 8 A proposed model of LA.EVs protect against aflatoxin B1-induced inflammatory intestinal injury by remodelling the gut microbiota and activating intestinal AHR/IL-22 signalling in mice

Abbreviations

AFB1	Aflatoxin B1
LA	*Lactobacillus amylovorus*
EVs	Extracellular vesicles
LA.EVs	*Lactobacillus amylovorus*-derived EVs
GM	Gut microbiota
MRS	Man, Rogosa, and Sharpe
ABX	Antibiotics
IAA	Indole-3-acetic acid
AHR	Aryl hydrocarbon receptor
IL-22	Interleukin-22

Supplementary Information

The online version contains supplementary material available at https://doi.org/10.1186/s12951-024-02979-3.

Supplementary Material 1

Acknowledgements

The study was supported by the National Natural Science Foundation of China (32102741), Natural Science Foundation of Jiangsu Province (BK20210399) and the Fundamental Research Funds for the Central Universities (Grant No.KJYQ2024010; KYT2023004).

Author contributions

JL performed most of the experiments, analyzed and interpreted the data, and wrote the manuscript; MS, YW, JL, SL, WK, XL provided technical support and performed the experiments; XC and KH contributed to the critical discussion of the project; YL conceived, designed, and supervised the study and wrote and critically revised the manuscript.

Data availability

The data that support the findings of the study are available from the corresponding author upon reasonable request.

Declarations

Ethics approval and consent to participate

Protocols of animal experiments included in this study were approved by Nanjing Agricultural University under the Laboratory Animal Care Ethics Committee for animal experiments (NJAU. No 20210624093). Informed consent was obtained from all individual participants.

Consent for publication

All authors consent to the publication of the article.

Competing interests

The authors declare no competing interests.

Received: 18 November 2023 / Accepted: 4 November 2024
Published online: 11 November 2024

References

1. Zhang N-Y, Qi M, Zhao L, Zhu M-K, Guo J, Liu J, Gu C-Q, Rajput SA, Krumm CS, Qi D-S, Sun L-H. Curcumin prevents aflatoxin B_1 hepatoxicity by inhibition of cytochrome P450 isozymes in Chick Liver. Toxins 2016;8.
2. Cheng L, Qin Y, Hu X, Ren L, Zhang C, Wang X, Wang W, Zhang Z, Hao J, Guo M, et al. Melatonin protects in vitro matured porcine oocytes from toxicity of aflatoxin B1. J Pineal Res. 2019;66:e12543.
3. Pauletto M, Giantin M, Tolosi R, Bassan I, Barbarossa A, Zaghini A, Dacasto M. Discovering the Protective effects of Resveratrol on aflatoxin B1-Induced

toxicity: a whole transcriptomic study in a bovine hepatocyte cell line. Antioxidants; 2021. p. 10. (Basel, Switzerland).
4. Pang VF, Chiang C-F, Chang C-C. The in vitro effects of aflatoxin B1 on physiological functions of swine alveolar macrophages. Veterinary Med Sci. 2020;6:919–25.
5. Yang C, Song G, Lim W. Effects of mycotoxin-contaminated feed on farm animals. J Hazard Mater. 2020;389:122087.
6. Liew W-P-P, Mohd-Redzwan S. Mycotoxin: its impact on Gut Health and Microbiota. Front Cell Infect Microbiol. 2018;8:60.
7. Akbari P, Braber S, Varasteh S, Alizadeh A, Garssen J, Fink-Gremmels J. The intestinal barrier as an emerging target in the toxicological assessment of mycotoxins. Arch Toxicol. 2017;91:1007–29.
8. Taranu I, Marin DE, Palade M, Pistol GC, Chedea VS, Gras MA, Rotar C. Assessment of the efficacy of a grape seed waste in counteracting the changes induced by aflatoxin B1 contaminated diet on performance, plasma, liver and intestinal tissues of pigs after weaning. Toxicon: Official J Int Soc Toxinology. 2019;162:24–31.
9. Contreras BG, De Vuyst L, Devreese B, Busanyova K, Raymaeckers J, Bosman F, Sablon E, Vandamme EJ. Isolation, purification, and amino acid sequence of lactobin A, one of the two bacteriocins produced by Lactobacillus amylovorus LMG P-13139. Appl Environ Microbiol. 1997;63:13–20.
10. Xu Z, He H, Zhang S, Guo T, Kong J. Characterization of Feruloyl Esterases produced by the four Lactobacillus species: L. Amylovorus, L. Acidophilus, L. Farciminis and L. Fermentum, isolated from Ensiled Corn Stover. Front Microbiol. 2017;8:941.
11. Sunmola AA, Ogbole OO, Faleye TOC, Adetoye A, Adeniji JA, Ayeni FA. Antiviral potentials of Lactobacillus plantarum, Lactobacillus amylovorus, and Enterococcus hirae against selected Enterovirus. Folia Microbiol. 2019;64:257–64.
12. Finamore A, Roselli M, Imbinto A, Seeboth J, Oswald IP, Mengheri E. Lactobacillus amylovorus inhibits the TLR4 inflammatory signaling triggered by enterotoxigenic Escherichia coli via modulation of the negative regulators and involvement of TLR2 in intestinal Caco-2 cells and pig explants. PLoS ONE. 2014;9:e94891.
13. Chew JRJ, Chuah SJ, Teo KYW, Zhang S, Lai RC, Fu JH, Lim LP, Lim SK, Toh WS. Mesenchymal stem cell exosomes enhance periodontal ligament cell functions and promote periodontal regeneration. Acta Biomater. 2019;89:252–64.
14. Margolis L, Sadovsky Y. The biology of extracellular vesicles: the known unknowns. PLoS Biol. 2019;17:e3000363.
15. Rabiei N, Ahmadi Badi S, Ettehad Marvasti F, Nejad Sattari T, Vaziri F, Siadat SD. Induction effects of Faecalibacterium prausnitzii and its extracellular vesicles on toll-like receptor signaling pathway gene expression and cytokine level in human intestinal epithelial cells. Cytokine. 2019;121:154718.
16. Liang L, Yang C, Liu L, Mai G, Li H, Wu L, Jin M, Chen Y. Commensal bacteria-derived extracellular vesicles suppress ulcerative colitis through regulating the macrophages polarization and remodeling the gut microbiota. Microb Cell Fact. 2022;21:88.
17. Macia L, Nanan R, Hosseini-Beheshti E, Grau GE. Host- and microbiota-derived extracellular vesicles, Immune function, and Disease Development. Int J Mol Sci. 2019;21.
18. Shen Q, Huang Z, Ma L, Yao J, Luo T, Zhao Y, Xiao Y, Jin Y. Extracellular vesicle miRNAs promote the intestinal microenvironment by interacting with microbes in colitis. Gut Microbes. 2022;14:2128604.
19. Bian X, Wu W, Yang L, Lv L, Wang Q, Li Y, Ye J, Fang D, Wu J, Jiang X, et al. Administration of Akkermansia muciniphila ameliorates Dextran Sulfate Sodium-Induced Ulcerative Colitis in mice. Front Microbiol. 2019;10:2259.
20. Singh R, Chandrashekharappa S, Bodduluri SR, Baby BV, Hegde B, Kotla NG, Hiwale AA, Saiyed T, Patel P, Vijay-Kumar M, et al. Enhancement of the gut barrier integrity by a microbial metabolite through the Nrf2 pathway. Nat Commun. 2019;10:89.
21. Pernomian L, Duarte-Silva M, de Barros Cardoso CR. The Aryl Hydrocarbon receptor (AHR) as a potential target for the Control of Intestinal Inflammation: insights from an Immune and Bacteria sensor receptor. Clin Rev Allergy Immunol. 2020;59:382–90.
22. Sun M, Ma N, He T, Johnston LJ, Ma X. Tryptophan (Trp) modulates gut homeostasis via aryl hydrocarbon receptor (AhR). Crit Rev Food Sci Nutr. 2020;60:1760–8.
23. Lin L, Liu Y, Chen L, Dai Y, Xia Y. Discovery of Norisoboldine Analogue III11 as a Novel and Potent Aryl Hydrocarbon receptor agonist for the treatment of Ulcerative Colitis. J Med Chem. 2023;66:6869–88.
24. Wang J, Wang P, Tian H, Tian F, Zhang Y, Zhang L, Gao X, Wang X. Aryl hydrocarbon receptor/IL-22/Stat3 signaling pathway is involved in the modulation of intestinal mucosa antimicrobial molecules by commensal microbiota in mice. Innate Immun. 2018;24:297–306.
25. Pinto CJG, Ávila-Gálvez MÁ, Lian Y, Moura-Alves P, Nunes Dos Santos C. Targeting the aryl hydrocarbon receptor by gut phenolic metabolites: a strategy towards gut inflammation. Redox Biol. 2023;61:102622.
26. Scott SA, Fu J, Chang PV. Microbial tryptophan metabolites regulate gut barrier function via the aryl hydrocarbon receptor. Proc Natl Acad Sci USA. 2020;117:19376–87.
27. Geng S, Cheng S, Li Y, Wen Z, Ma X, Jiang X, Wang Y, Han X. Faecal microbiota transplantation reduces susceptibility to Epithelial Injury and modulates Tryptophan Metabolism of the Microbial Community in a Piglet Model. Volume 12. Journal of Crohn's & Colitis; 2018. pp. 1359–74.
28. Gu YZ, Hogenesch JB, Bradfield CA. The PAS superfamily: sensors of environmental and developmental signals. Annu Rev Pharmacol Toxicol. 2000;40:519–61.
29. Lee JS, Cella M, McDonald KG, Garlanda C, Kennedy GD, Nukaya M, Mantovani A, Kopan R, Bradfield CA, Newberry RD, Colonna M. AHR drives the development of gut ILC22 cells and postnatal lymphoid tissues via pathways dependent on and independent of Notch. Nat Immunol. 2011;13:144–51.
30. Qiu J, Heller JJ, Guo X, Chen Z-mE, Fish K, Fu Y-X, Zhou L. The aryl hydrocarbon receptor regulates gut immunity through modulation of innate lymphoid cells. Immunity. 2012;36.
31. Grau KR, Zhu S, Peterson ST, Helm EW, Philip D, Phillips M, Hernandez A, Turula H, Frasse P, Graziano VR, et al. The intestinal regionalization of acute norovirus infection is regulated by the microbiota via bile acid-mediated priming of type III interferon. Nat Microbiol. 2020;5:84–92.
32. Shi Z, Li X, Zhang Y-M, Zhou Y-Y, Gan X-F, Fan Q-Y, He C-Q, Shi T, Zhang S-Y. Constitutive androstane receptor (CAR) mediates pyrene-induced inflammatory responses in mouse liver, with increased serum amyloid A proteins and Th17 cells. Br J Pharmacol. 2022;179:5209–21.
33. Russell WR, Duncan SH, Scobbie L, Duncan G, Cantlay L, Calder AG, Anderson SE, Flint HJ. Major phenylpropanoid-derived metabolites in the human gut can arise from microbial fermentation of protein. Mol Nutr Food Res. 2013;57:523–35.
34. Rodrigues I, Naehrer K. A three-year survey on the worldwide occurrence of mycotoxins in feedstuffs and feed. Toxins. 2012;4:663–75.
35. Xu Q, Shi W, Lv P, Meng W, Mao G, Gong C, Chen Y, Wei Y, He X, Zhao J, et al. Critical role of caveolin-1 in aflatoxin B1-induced hepatotoxicity via the regulation of oxidation and autophagy. Cell Death Dis. 2020;11:6.
36. Sergent T, Ribonnet L, Kolosova A, Garsou S, Schaut A, De Saeger S, Van Peteghem C, Larondelle Y, Pussemier L, Schneider Y-J. Molecular and cellular effects of food contaminants and secondary plant components and their plausible interactions at the intestinal level. Food Chem Toxicology: Int J Published Br Industrial Biol Res Association. 2008;46:813–41.
37. Akinrinmade FJ, Akinrinde AS, Amid A. Changes in serum cytokine levels, hepatic and intestinal morphology in aflatoxin B1-induced injury: modulatory roles of melatonin and flavonoid-rich fractions from Chromolena odorata. Mycotoxin Res. 2016;32:53–60.
38. Chen J, Lv Z, Cheng Z, Wang T, Li P, Wu A, Nepovimova E, Long M, Wu W, Kuca K. Bacillus amyloliquefaciens B10 inhibits aflatoxin B1-induced cecal inflammation in mice by regulating their intestinal flora. Food Chem Toxicology: Int J Published Br Industrial Biol Res Association. 2021;156:112438.
39. Wang X, Yang F, Na L, Jia M, Ishfaq M, Zhang Y, Liu M, Wu C. Ferulic acid alleviates AFB1-induced duodenal barrier damage in rats via up-regulating tight junction proteins, down-regulating ROCK, competing CYP450 enzyme and activating GST. Ecotoxicol Environ Saf. 2022;241:113805.
40. Romero A, Ares I, Ramos E, Castellano V, Martínez M, Martínez-Larrañaga M-R, Anadón A, Martínez M-A. Mycotoxins modify the barrier function of Caco-2 cells through differential gene expression of specific claudin isoforms: protective effect of illite mineral clay. Toxicology. 2016;353–4:21–33.
41. Zhang M, Li Q, Wang J, Sun J, Xiang Y, Jin X. Aflatoxin B1 disrupts the intestinal barrier integrity by reducing junction protein and promoting apoptosis in pigs and mice. Ecotoxicol Environ Saf. 2022;247:114250.
42. Morishita M, Horita M, Higuchi A, Marui M, Katsumi H, Yamamoto A. Characterizing different probiotic-derived extracellular vesicles as a Novel adjuvant for Immunotherapy. Mol Pharm. 2021;18:1080–92.
43. Woith E, Fuhrmann G, Melzig MF. Extracellular vesicles-connecting kingdoms. Int J Mol Sci. 2019;20.
44. Bitto NJ, Kaparakis-Liaskos M. The therapeutic benefit of bacterial membrane vesicles. Int J Mol Sci. 2017;18.
45. Hynönen U, Kant R, Lähteinen T, Pietilä TE, Beganović J, Smidt H, Uroić K, Avall-Jääskeläinen S, Palva A. Functional characterization of probiotic surface

layer protein-carrying Lactobacillus amylovorus strains. BMC Microbiol. 2014;14:199.
46. Marti R, Dabert P, Ziebal C, Pourcher A-M. Evaluation of Lactobacillus sobrius/L. Amylovorus as a new microbial marker of pig manure. Appl Environ Microbiol. 2010;76:1456–61.
47. Shen J, Zhang J, Zhao Y, Lin Z, Ji L, Ma X. Tibetan pig-derived probiotic Lactobacillus amylovorus SLZX20-1 improved intestinal function via producing enzymes and regulating intestinal Microflora. Front Nutr. 2022;9:846991.
48. Inczefi O, Bacsur P, Resál T, Keresztes C, Molnár T. The influence of Nutrition on Intestinal Permeability and the Microbiome in Health and Disease. Front Nutr. 2022;9:718710.
49. Liu S, Li J, Kang W, Li Y, Ge L, Liu D, Liu Y, Huang K. Aflatoxin B1 induces intestinal barrier dysfunction by regulating the FXR-Mediated MLCK Signaling Pathway in mice and in IPEC-J2 cells. J Agric Food Chem. 2023;71:867–76.
50. Xu P, Dong S, Luo X, Wei B, Zhang C, Ji X, Zhang J, Zhu X, Meng G, Jia B, Zhang J. Humic acids alleviate aflatoxin B1-induced hepatic injury by reprogramming gut microbiota and absorbing toxin. Ecotoxicol Environ Saf. 2023;259:115051.
51. Yang A-M, Lin C-Y, Liu S-H, Syu G-D, Sun H-J, Lee K-C, Lin H-C, Hou M-C. Saccharomyces Boulardii ameliorates non-alcoholic steatohepatitis in mice Induced by a methionine-choline-deficient Diet through Gut-Liver Axis. Front Microbiol. 2022;13:887728.
52. Camilleri M, Madsen K, Spiller R, Greenwood-Van Meerveld B, Verne GN. Intestinal barrier function in health and gastrointestinal disease. Neurogastroenterol Motil. 2012;24:503–12.
53. Groschwitz KR, Hogan SP. Intestinal barrier function: molecular regulation and disease pathogenesis. J Allergy Clin Immunol. 2009;124.
54. Chen P, Stärkel P, Turner JR, Ho SB, Schnabl B. Dysbiosis-induced intestinal inflammation activates tumor necrosis factor receptor I and mediates alcoholic liver disease in mice. Hepatology (Baltimore MD). 2015;61:883–94.
55. Robert H, Payros D, Pinton P, Théodorou V, Mercier-Bonin M, Oswald IP. Impact of mycotoxins on the intestine: are mucus and microbiota new targets? J Toxicol Environ Health Part B Crit Reviews. 2017;20:249–75.
56. Elmassry MM, Zayed A, Farag MA. Gut homeostasis and microbiota under attack: impact of the different types of food contaminants on gut health. Crit Rev Food Sci Nutr. 2022;62:738–63.
57. Fonseca A, Kenney S, Van Syoc E, Bierly S, Dini-Andreote F, Silverman J, Boney J, Ganda E. Investigating antibiotic free feed additives for growth promotion in poultry: effects on performance and microbiota. Poult Sci. 2024;103:103604.
58. Liu S, Kang W, Mao X, Ge L, Du H, Li J, Hou L, Liu D, Yin Y, Liu Y, Huang K. Melatonin mitigates aflatoxin B1-induced liver injury via modulation of gut microbiota/intestinal FXR/liver TLR4 signaling axis in mice. J Pineal Res. 2022;73:e12812.
59. Liu Y, Li J, Kang W, Liu S, Liu J, Shi M, Wang Y, Liu X, Chen X, Huang K. Aflatoxin B1 induces liver injury by disturbing gut microbiota-bile acid-FXR axis in mice. Food Chem Toxicology: Int J Published Br Industrial Biol Res Association. 2023;176:113751.
60. Mao T, Su C-W, Ji Q, Chen C-Y, Wang R, Vijaya Kumar D, Lan J, Jiao L, Shi HN. Hyaluronan-induced alterations of the gut microbiome protects mice against Citrobacter rodentium infection and intestinal inflammation. Gut Microbes. 2021;13:1972757.
61. Jin X, You L, Qiao J, Han W, Pan H. Autophagy in colitis-associated colon cancer: exploring its potential role in reducing initiation and preventing IBD-Related CAC development. Autophagy. 2024;20:242–58.
62. Roager HM, Licht TR. Microbial tryptophan catabolites in health and disease. Nat Commun. 2018;9:3294.
63. Bansal T, Alaniz RC, Wood TK, Jayaraman A. The bacterial signal indole increases epithelial-cell tight-junction resistance and attenuates indicators of inflammation. Proc Natl Acad Sci USA. 2010;107:228–33.
64. Shimada Y, Kinoshita M, Harada K, Mizutani M, Masahata K, Kayama H, Takeda K. Commensal bacteria-dependent indole production enhances epithelial barrier function in the colon. PLoS ONE. 2013;8:e80604.
65. Albillos A, de Gottardi A, Rescigno M. The gut-liver axis in liver disease: pathophysiological basis for therapy. J Hepatol. 2020;72:558–77.
66. Wu L, Tang Z, Chen H, Ren Z, Ding Q, Liang K, Sun Z. Mutual interaction between gut microbiota and protein/amino acid metabolism for host mucosal immunity and health. Anim Nutr (Zhongguo Xu Mu Shou Yi Xue Hui). 2021;7:11–6.
67. Lamas B, Richard ML, Leducq V, Pham H-P, Michel M-L, Da Costa G, Bridonneau C, Jegou S, Hoffmann TW, Natividad JM, et al. CARD9 impacts colitis by altering gut microbiota metabolism of tryptophan into aryl hydrocarbon receptor ligands. Nat Med. 2016;22:598–605.
68. Natividad JM, Agus A, Planchais J, Lamas B, Jarry AC, Martin R, Michel M-L, Chong-Nguyen C, Roussel R, Straube M et al. Impaired aryl hydrocarbon receptor ligand production by the gut microbiota is a key factor in metabolic syndrome. Cell Metabol. 2018;28.
69. Zelante T, Iannitti RG, Cunha C, De Luca A, Giovannini G, Pieraccini G, Zecchi R, D'Angelo C, Massi-Benedetti C, Fallarino F, et al. Tryptophan catabolites from microbiota engage aryl hydrocarbon receptor and balance mucosal reactivity via interleukin-22. Immunity. 2013;39:372–85.

Publisher's note